Cu(II) Complexes Conjugated with 9-Aminoacridine Intercalator: Their Binding Modes to DNA and Activities as Chemical Nuclease

Jung Hee Kim,[†,*] **Mi Ryung Youn, Young-Ae Lee, Jong Moon Kim, and Seog K. Kim**[*]

[†]*Department of Chemistry, Sun Moon University, Chungnam, Asan 336-708, Korea.* [*]*E-mail: junghee@sunmoon.ac.kr*
Department of Chemistry, Yeungnam University, Gyeong-buk, Gyeongsan 712-749, Korea. [*]*E-mail: seogkim@yu.ac.kr*
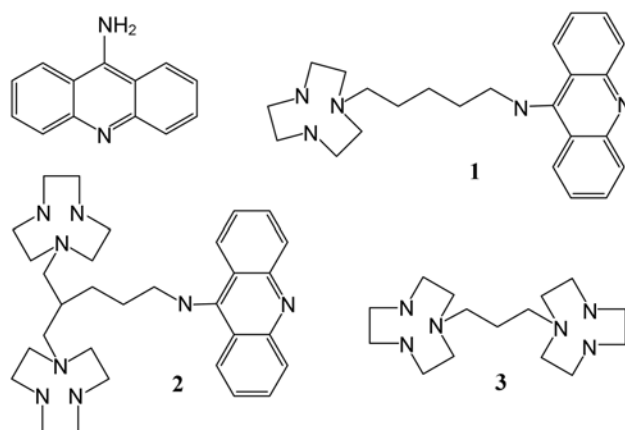*Received October 17, 2006*

New *mono-* and *bis*-Cu(II)-triazacyclononane(tacn) complex that conjugated with 9-aminoacridine were synthesized, and their binding modes and DNA cleavage activity were investigated in this study. When the classic intercalator, 9-aminoacridine, was conjugated to *mono-* and *bis*-Cu(II)-tacn complexes, a significant red-shift and hypochromism in absorption spectrum was apparent in the acridine absorption region upon binding to DNA. Furthermore, the magnitude of the negative reduced linear dichroism signal in the substrate absorption region appeared to be larger than that in the DNA absorption region. These spectral observations indicated that the acridine moiety intercalated when the Cu(II)-tacn complex was conjugated. In contrast, from a close analysis of the circular and linear dichroism spectrum, the aminoacridine-free *bis*-Cu(II)-tacn complex was concluded to bind at the phosphate groups of DNA. The 9-aminoacridine-free-*bis*-Cu(II)-tacn complex produces the nicked and linear DNA. On the other hand, 9-aminoacridine conjugated *mono-*and *bis*-Cu(II)-tacn complexes showed unspecific binding with negligible DNA cleavage.

Key Words : Cu complex, DNA cleavage, Acridine, Linear dichroism, Fluorescence

Introduction

The interactions of transition metal complexes with DNA have been extensively studied for their usage as probes for DNA structure and their potential application to chemotherapy.[1-4] One of the important DNA related activity of the transition metal complexes is that some of the complexes show the ability to cleave DNA. There have been substantial efforts to introduce high structure and/or sequence selectivity as well as to enhance the nuclease activity by making rational changes in the ligand structures of the metal complexes. Since the first report that a mixture of phenanthroline, Cu(II) and thiol could cut the poly[d(A-T)$_2$],[5] a number of Cu(II) complex have been reported to be active in DNA strand scission.[6-14] For a recent instance, the binding mode and nuclease activity of the macrocyclic Cu(II) complex with different function groups have been reported.[8] Although the function group on the side chain of macrocycle played a key role in determining the binding mode, Cu complexes with different binding modes were found to cleave double-stranded DNA in the presence of 2-mercaptoethanol and H$_2$O$_2$. A tridentate Cu(II) complex, which has been suggested to intercalate by viscometric titration, has shown DNA cleavage activity in the presence of ascorbic acid or glutathione.[13] In the absence of any additive, a few tacn based mono- and binuclear Cu(II) complexes have been reported to be efficient in cleaving DNA phosphate backbone.[15-18]

In this study, we synthesized 9-aminoacridine conjugated with *mono-* and *bis*-Cu(II)-triazacyclononane (tacn) complexes (Scheme 1) and investigated their binding modes and activity as chemical nucleases. 9-Aminoacridine, an established intercalator,[19-21] serves as an anchor for the Cu(II)-tacn complexes.
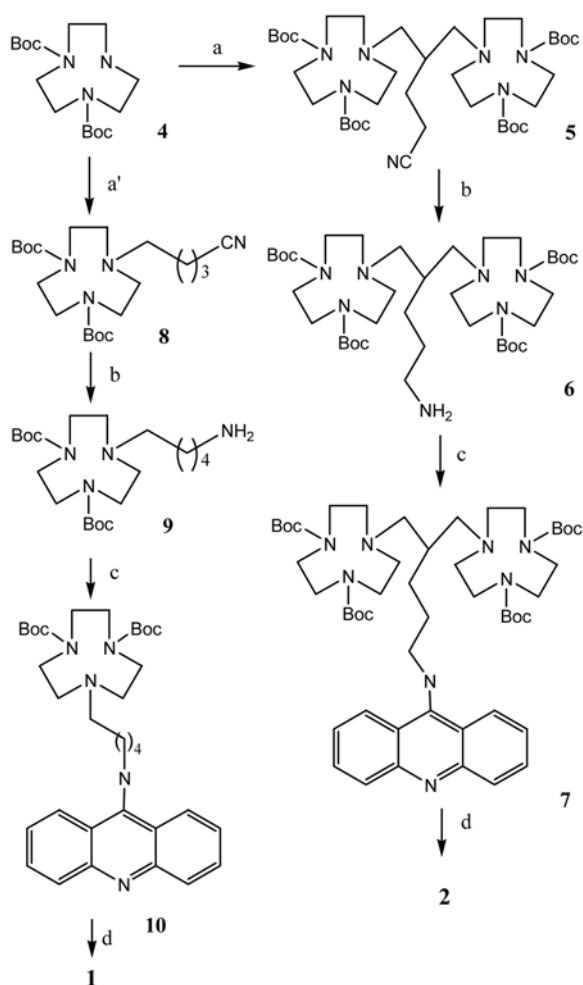

Scheme 1. Chemical structures of 9-aminoacridine, ligands 1, 2 and 3.

Materials and Methods

Chemicals. All chemicals were purchased from Sigma and used without further purification. Calf thymus DNA (DNA), purchased from Worthington Biochemical Co. (Lakewood, NJ), was dissolved in a 5 mM cacodylate buffer, pH 7.0, containing 100 mM NaCl and 1 mM ethylenediaminetetraacetic acid (EDTA) at 4 °C. The DNA solution was then dialyzed several times against 10 mM 4-(2-hydroxyethyl)piperazine-1-ethanosulfonic acid (HEPES) buffer pH 7.0. Supercoiled pCMV-Myc DNA was purchased from Clonetech. Labs (Mountain View, CA). The concentration of DNA was determined using extinction coefficient $\varepsilon_{258nm} = 6700$ M^{-1}cm^{-1} and hence this denotes the concentration in base.

Synthetic procedure. ^{1}H and ^{13}C NMR spectrum were

Scheme 2. a) 2-cyanoethyldibromopropane, a') 5-bromovaleronitrile, Et₃N, reflux, b) Raney/Ni, NH₄OH, c) phenoxyacridine, phenol, 80 °C, d) HCl/MeOH, aq. NaOH/CH₂Cl.

obtained from VARIAN UNITY-INOVA 300 MHz spectrometer. Mass spectra of the ligands and the intermediates were recorded on a Thermo Finnigan AQA Lc-Mass. All the chemicals used in the synthetic procedure except solvents were purchased from Aldrich. Ligands **1** and **2** were prepared from *tert*-butoxycarbonyl (Boc) protected tacn **4** according to Scheme 2. Ligand **3** was prepared according to literature procedure.[16]

5-(4,7-Di-*tert*-Boc-[1,4,7]triazonan-1-yl)-4-(4,7-di-*tert*-Boc-l-[1,4,7]triazonan-1-ylmethyl)-pentanenitrile (5): To di-*tert*-Boc-tacn **4** (3 g, 9.1 mmol) in 60 mL of acetonitrile was added 2-cyanoethyldibromopropane (1.16 g, 4.55 mmol) in the presence of triethylamine (1 g, 1.0 mmol). The reaction mixture was refluxed for two days and evaporated to dryness. The residue was dissolved in CH₂Cl₂ and extracted with water. The organic layer was dried with anhydrous Na₂SO₄, filtered and evaporated. After column chromatography (Hexane : EtOAc), **5** (2.8 g, 3.72 mmol) was obtained as a syrup (82%). ¹H NMR: 1.44 (s, 36H), 1.59-1.82 (m, 4H), 2.17-2.29 (m, 1H), 2.41-2.59 (m, 12H), 3.08-3.51 (m, 16H), ESI MS: m/z 752.3 for [MH]⁺ (Calcd. 751.52 for C₃₈H₆₉N₇O₈).

5-(4,7-Di-*tert*-Boc-[1,4,7]triazonan-1-yl)-4-(4,7-di-*tert*-Boc-[1,4,7]triazonan-1-ylmethyl)-pentylamine (6): To **5** (1.4 g, 1.86 mmol) and 5 mL of aqueous NH₄OH in 50 mL EtOH was added 2 g of activated Raney Ni. The solution was stirred under hydrogen pressure (50 psi) until no more starting material left. The mixture was filtered on celite and the filtrate was evaporated to dryness. The residue was dissolved in CH₂Cl₂ and extracted with 0.1 N NaOH. The organic layer was dried over anhydrous Na₂CO₃ and evaporated to dryness to give **6** (1.2 g, 1.58 mmol) as white solids (85%). ¹H NMR (CDCl₃): 1.43 (bs, 40H), 1.67-1.75 (m, 1H), 2.19-2.67 (m, 12H), 2.88-2.95 (m, 2H), 3.19-3.46 (m, 16H), ESI MS: m/z 756.2 [MH]⁺ (Calcd. 755.55 C₃₈H₇₃N₇O₈).

Acridin-9-yl-[5-(4,7-di-*tert*-Boc-[1,4,7]triazonan-1-yl)-4-(4,7-di-*tert*-Boc-[1,4,7]triazonan-1-ylmethyl)-pentyl]-amine (7): 9-Chloroacridine (142 mg, 0.66 mmol) with phenol (1 g) was placed in 70 °C oil bath for 1 hr. To above solution, **6** (500 mg, 0.66 mmol) in 50 °C phenol (2 g) was added and heated up to 80 °C for 2 hr. The mixture was cooled to room temperature. After column chromatography (CH₂Cl₂ : MeOH : Et₃N = 90 : 9.5 : 0.5), **7** (200 mg, 0.21 mmol) was obtained as a yellowish syrup (32%). ¹H NMR (CDCl₃): 1.44-1.48 (3s, 36H), 1.81-1.93 (m, 2H), 2.19-2.63 (m, 10H), 3.12-3.63 (m, 14H), 3.86 (m, 2H), 7.34 (t, *J* = 7.6 Hz, 2H), 7.74 (t, *J* = 7.3 Hz, 2H) 8.08-8.22 (m, 2H), 8.28 (d, *J* = 8.9 Hz, 2H), ESI MS: m/z 933.2 [MH]⁺ (Calcd. 932.61 for C₅₁H₈₀N₈O₈).

Acridin-9-yl-(5-[1,4,7]triazonan-1-yl-4-[1,4,7]triazonan-1-ylmethyl-pentyl)-amine (2) **7** (160 mg, 0.17 mmol) was dissolved in 2 mL MeOH and HCl/MeOH (generated from acetylchloride and MeOH) was added slowly. After 3-4 hrs stirring at room temperature, a yellowish precipitate was formed, filtered and dried *in vacuo*. ¹H NMR (D₂O): 1.24 (m, 2H), 1.65 (m, 2H), 1.94 (m, 1H), 2.57 (t, *J* = 6.9 Hz, 4H), 2.84 (t, *J* = 5.3 Hz, 8H), 3.11 (m, 8H), 3.45 (s, 8H), 3.69 (t, *J* = 6.9 Hz, 2H), 7.14 (d, *J* = 8.2 Hz, 2H), 7.23 (dd, *J* = 8.0 Hz, 2H), 7.60 (dd, *J* = 7.5 Hz, 2H), 7.84 (d, *J* = 8.9 Hz, 2H), ¹³C NMR: 25.84, 28.17, 32.49, 42.39, 42.47, 43.98, 48.73, 58.03, 118.39, 124.07, 135.47, 157.54, ESI MS: m/z 533.2 for [MH]⁺ (Calcd. 532.40 for C₃₁H₄₈N₈).

The above HCl salt was dissolved in small amount of water and the pH of the solution was adjusted to 12 by adding solid NaOH. The solution was extracted by CH₂Cl₂ and dried with anhydrous Na₂CO₃. Evaporation to dryness gave **2** (87 mg, 0.16 mmol) in quantitative yield. The mononuclear ligand **1** was prepared as the same method in Scheme 2, except using 5-bromovaleronitrile in the synthesis of **8**.

7-(4-Cyano-butyl)-[1,4,7]triazonane-1,4-dicarboxylic acid di-*tert*-butyl ester (8): Di-*tert*-Boc-tacn **4** (1.1 g, 3.34 mmol) and 5-bromovaleronitrile (631 mg, 3.34 mmol) produced **8** (1.2 g, 2.92 mmol) as a colorless syrup (86%). ¹H NMR (CDCl₃): 1.51 (s, 18H), 1.56-1.78 (m, 6H), 2.36-2.45 (m, 2H), 2.5-2.62 (m, 2H), 2.62-2.70 (m, 2H), 3.25-3.34 (m, 4H), 3.41-3.54 (m, 4H), ESI MS: m/z 411.3 for [MH]⁺ (Calcd. 410.29 for C₂₁H₃₈N₄O₄).

7-(5-Amino-pentyl)-[1,4,7]triazonane-1,4-dicarboxylic acid di-*tert*-butyl ester (9): **8** (1.2 g, 2.92 mmol) gave **9** (1.1

g, 2.65 mmol) as a pale yellow syrup (91%). ^{1}H NMR (CDCl3): 1.26 (m, 2H), 1.40-1.51 (bs, 20H), 1.76 (bs, 2H), 2.46-2.51 (m, 2H), 2.59-2.64 (m, 4H), 2.67-2.71 (m, 2H), 3.22-3.29 (m, 4H), 3.43-3.49 (m, 4H). ESI MS: m/z 414.9. for [MH]$^+$ (Calcd. 414.32 for $C_{21}H_{42}N_4O_4$).

7-[5-(Acridin-9-ylamino)-pentyl]-[1,4,7]triazonane-1,4-dicarboxylic acid di-*tert*-butyl ester (10): 9-Chloroacridine (200 mg, 0.93 mmol) and **9** (385 mg, 0.93 mmol) produced 266 mg of **10** as yellowish syrup (45%). ^{1}H NMR (CDCl3): 1.46 (s, 18H), 1.85 (m, 2H), 2.47 (t, *J* = 6.0 Hz, 2H), 2.60 (m, 4H), 3.25-3.28 (m, 4H), 3.40-3.48 (m, 4H), 3.88 (t, *J* = 7.0 Hz, 2H), 7.31 (t, 7.6 Hz, 2H), 7.61 (t, *J* = 7.6 Hz, 2H), 8.06 (d, *J* = 7.5 Hz, 2H), 8.17 (d, *J* = 8.7 Hz, 2H), ESI MS: m/z 592.2 [MH]$^+$ (Calcd. 591.38 for $C_{34}H_{49}N_5O_4$) ESI MS: m/z 592.2 for [MH]$^+$ (Calcd. 591.38 for $C_{34}H_{49}N_5O_4$).

Acridin-9-yl-(5-[1,4,7]triazonan-1-yl-pentyl)-amine (1): **1**·HCl salt was obtained from **10** in quantitative yield. ^{1}H NMR (D2O): 1.16 (q, *J* = 7.35 Hz, 2H), 1.42-1.58 (m, 6H), 2.75 (dt, *J* = 7.5 Hz, 2H), 3.03 (t, *J* = 5.4 Hz, 4H), 3.21 (t, *J* = 5.6 Hz, 4H), 3.35 (t, *J* = 7.35 Hz, 2H), 3.37 (s, 4H), 6.89 (d, *J* = 8.3 Hz, 2H), 7.04 (dd, *J* = 7.7 Hz, 2H), 7.43 (dd, *J* = 7.7 Hz, 2H), 7.52 (d, *J* = 8.8 Hz, 2H), ^{13}C NMR: 23.55, 23.88, 28.93, 42.09, 43.08, 47.96, 48.83, 55.20, 118.2, 123.85, 135.28, 157.34, ESI MS: m/z 392.2 [MH]$^+$ (Calcd. 391.27 for $C_{24}H_{33}N_5$).

1-[Cu(II)]2(NO3)4 xH2O and 2-Cu(II)(NO3)2 xH2O. Cu(II) complexes of **1** and **2** were prepared by mixing ethanolic solution of the ligand and 2.0 or 1.0 equivalent of Cu(NO3)2, respectively. The resulting precipitate was filtered, washed with cold ethanol, diethylether, and dried *in vacuo*. In general, The solution (5-100 μM) of L·xHCl (L = 1, 2, 3) and Cu(NO3)2 were prepared separately in an appropriate buffer and mixed just before use.

1-Cu(II)(NO3)2 xH2O: ESI MS: m/z 579 [M], 516 [M-NO3]

2-[Cu(II)]2(NO3)4 xH2O: ESI MS: m/z 659 [M-3(NO3)], 720 [M-2(NO3)]

Spectroscopic measurement. Absorption spectra were recorded on a Jasco V550 spectrophotometer (Tokyo, Japan). In the course of titration, small aliquots of the titrant were added to the sample solution and volume corrections were made. In general, binding of a substrate to DNA produces hypochromism, a broadening of the band and a red-shift in the substrate absorption region. When the binding mode is homogeneous, the ground state association constant for the drug-DNA complex formation may be estimated from the changes in absorbance at a fixed wavelength, using the Benesi-Hildebrand equation.[21]

$$\frac{1}{\Delta A} = -\frac{1}{(\varepsilon_b - \varepsilon_f)[L_t]} + \frac{1}{(\varepsilon_b - \varepsilon_f)[L_t]K_{BH}}\frac{1}{[DNA]}$$

Where ε is the extinction coefficient, the subscripts *b*, *f* and *t* denote bound, free and total drug, respectively. [L] is the substrate concentration and ΔA is the change in the absorbance at a given wavelength. By plotting the reciprocal absorbance with respect to the reciprocal concentration of DNA, the association constant for the complex formation can be calculated from the ratio of the slope to intercept. The

Benesi-Hildebrand plots were constructed by the changes in absorbance at 435 nm for 9-aminoacridine and at 450 nm for Cu-1 and Cu-2 complexes. Since Cu-3 complex does not absorb radiation in the UV/visible (UV/vis) region, this approach is not applicable.

The linear dichroism spectrum (LD) is defined to be the differential absorption spectrum of the light polarized parallel and perpendicular to the laboratory reference axis.[22-24] In the case of flow LD, the parallel direction is the flow direction. Measured LD is then divided by the isotropic absorption spectrum to give a reduced LD (LD^r). The LD^r in the absorption region of the intercalated drug, corresponding in-plane $\pi \rightarrow \pi^*$ transition, is negative and the magnitude is larger or comparable to that in the DNA absorption region, while the LD^r signal is positive for drugs bound at the minor groove. The LD spectra of the oriented sample were measured by a Jasco J715 spectropolarimeter. The orientation of the DNA complexes was achieved using a flow Couette cell with an inner rotating cylinder. The path length of the light of the Couette cell is 1 mm.
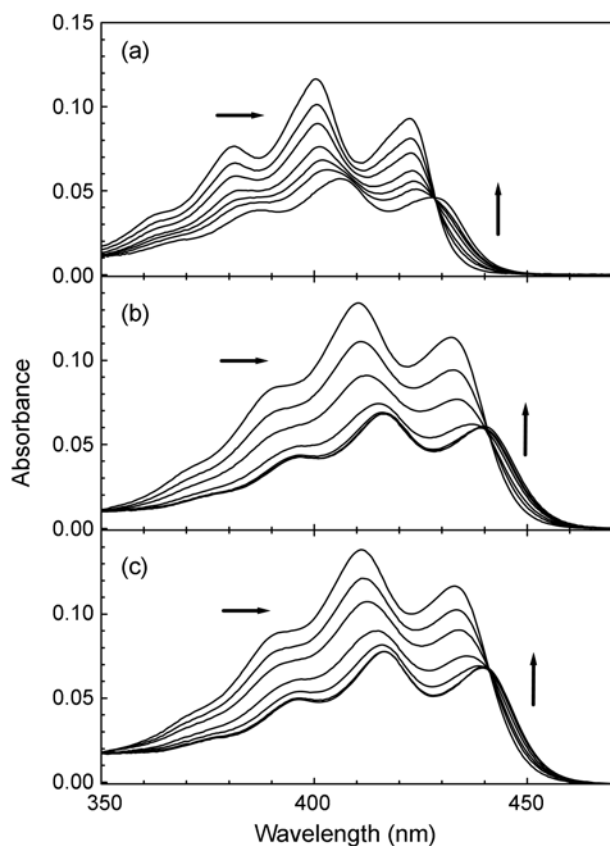
Steady state fluorescence measurement was performed on a Jasco FP777 fluorometer and fluorescence decay time on an IBH 5000U Fluorescence Life Time System (Glasgow, UK). The LED source of a nano LED-07, which produces an excitation radiation at 404 nm with full width at a half maximum of ~1.3 ns, was used to excite the DNA complexes. The slit width for both excitation and emission was 4 nm.

DNA cleavage experiments. Stock solutions of 0.1 mM Cu(NO3)2, 9-aminoacridine and L·xHCl were prepared separately in 10 mM HEPES (pH 7.3). For the cleavage reaction, Cu(NO3)2 solution and the ligand solution was mixed and incubated 30 min before use. Appropriate amounts of supercoiled pCMV-Myc DNA and the ligand or ligand-Cu(II) solutions were mixed at ice bath. The final volume was adjusted to 20-40 μL by adding appropriate volumes of the buffer solution. In the presence or absence of Cu(II) ion, the final concentrations of the 9-aminoacridine, **1**, **2**, and **3** in the incubating solution were 0-50 μM, and that of DNA was 1.54 μg/20 μL, corresponding to 114 μM in base. About 4-5 mL of an aliquot was placed in an eppendorf tube and incubated at 30(±0.5) ⁰C. At certain time intervals, the reaction was stopped by adding gel loading buffer (0.2% bromophenol blue, 0.2% xylene cyanol, 50% glycerol) containing 4 mM EDTA, and stored at −20 ⁰C until analysis. Cleavage products were analyzed in 1% agarose gels. The gels were staining in TAE buffer containing 1 mg/mL ethidium bromide and DNA degradation was determined by Kodak 1D Image Analysis software. The intensity correction factor of 1.22 for supercoiled DNA (form I) obtained from the calibration experiments was utilized.[16] All experiments were performed in triplicate. The kinetic run by gel electrophoresis was reproducible within 20% error.

Results

Absorption and fluorescence measurement of the Cu-1 and Cu-2. The absorption spectra of 9-aminoacridine, and
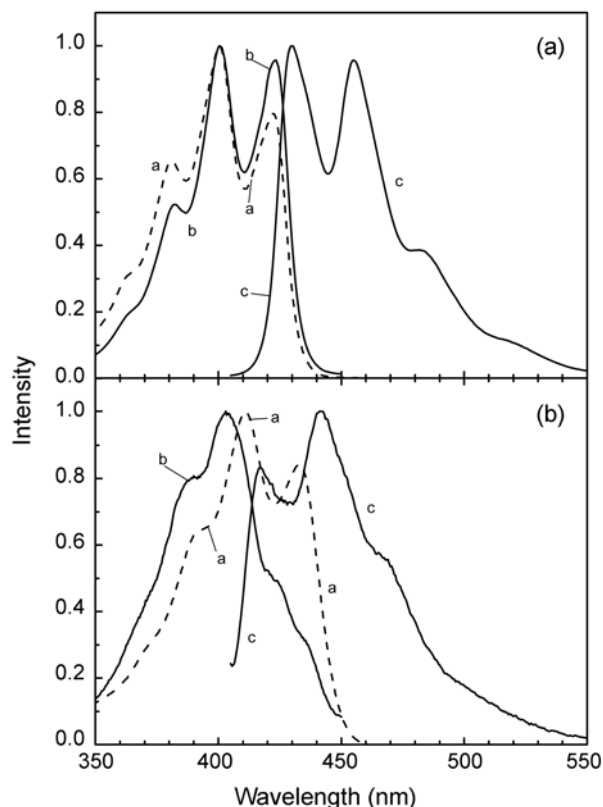
Cu-1 and Cu-2 complexes in the absence and the presence of DNA are depicted in Figure 1 panel a, b and c, respectively. In the absence of DNA, 9-aminoacridine shows its maximum absorbance at 381 nm, 400 nm and 422 nm. The absorption spectra of Cu-1 and Cu-2 complexes are similar in the absence of DNA, displaying the maximums at 392 nm, 410 nm and 432 nm for Cu-1 complex and at 393 nm, 411 nm and 433 nm for Cu-2 complex. Attachment of Cu(II)-tacn to 9-aminoacridine results in a 10 nm-11 nm red-shift, suggesting that there is an interaction between them. As the concentration of DNA increased, a red-shift in the absorption envelope and hypochromism are apparent for all three compounds. In the 9-aminoacridine, the red-shift is 6 nm and hypochromism is *ca.* 51% at the lowest energy absorption band in the presence of 100 μM of DNA. For both Cu-1 and Cu-2 complexes, a 6-7 nm red-shift for all absorption bands is produced. The hypochromism is *ca.* 45% for Cu-1 complex and *ca.* 40% for Cu-2 complex in the presence of 100 μM of DNA. This observation suggests that the extent of spectral changes for all three compounds is similar in the presence of DNA, suggesting that they all associate with DNA through a similar binding mode. The Benesi-Hildebrand plot is constructed from the change in absorbance at 435 nm for 9-aminoacridine and at 450 nm for Cu-1 and Cu-2 complexes (data not shown). The association constants are obtained from the ratio of the slope to intercept as (1.3 ± 0.2)
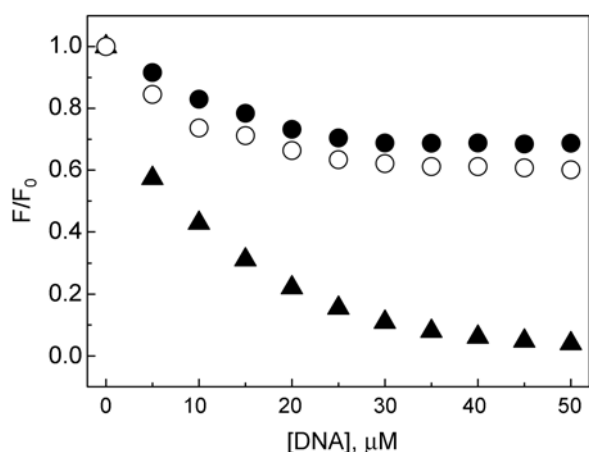
$\times 10^4$ M^{-1} for 9-aminoacridine and $(0.6 \pm 0.3) \times 10^4$ M^{-1} for Cu-1 and Cu-2 complexes. Cu-1 and Cu-2 complexes exhibited similar association constants. The association constant for the 9-aminoacridine-DNA complex formation has been reported at about one order higher than the value reported in this work by fluorescence titration.[21]

Fluorescence excitation and emission spectra of 9-aminoacridine and Cu-2 complex are compared in Figure 2. The overall fluorescence spectrum of Cu-1 complex resembles that of Cu-2 complex, although very small differences are noticed and therefore, it is not shown for reasons of clarity. In addition to changes in the absorption spectrum, the presence of the Cu(II)-tacn alters the properties of both the fluorescence excitation and emission spectra of Cu-1 and Cu-2 complexes significantly. In comparison with 9-aminoacridine, whose absorption and excitation spectrum do not significantly change, the excitation spectra of Cu-1 and Cu-2 complexes exhibit blue-shift and the vibronic structures crumble. Similar crumbles in vibronic structure and blue-shift are observed for the fluorescence emission spectrum, suggesting that the excited state of both Cu-1 and Cu-2 complexes in aqueous solution is quite different from that at the ground state. The decrease in quantum yield also is very significant. The relative quantum yield of Cu-1 and Cu-2

Figure 1. Absorption titration of 9-aminoacridine (panel a), Cu-1 (panel b), and Cu-2 (panel c). [substrate] = 10 μM. DNA concentrations are 0, 10, 20, 30, 40, 50, 100 μM to the arrow direction.

Figure 2. Normalized absorption (dashed, curve a), fluorescence excitation (solid, curve b) and emission spectra (solid, curve c) of 9-aminoacridine (panel a) and Cu-2 (panel b) in 10 mM HEPES buffer. [substrate] = 1 μM. Those of Cu-1 are similar to those of Cu-2. The excitation spectrum is recorded through a 457 nm emission window and the emission spectrum at 400 nm excitation. Slit widths are 3/3 nm for both excitation and emission spectra.
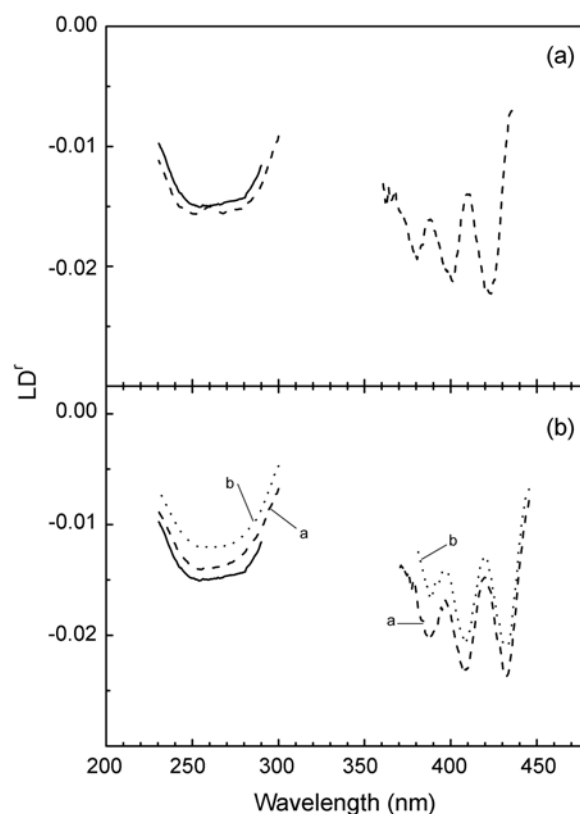
Figure 3. Decreases in the relative fluorescence intensity of Cu-1 (open circles) and Cu-2 (closed circle) with respect to increasing DNA concentration. Excitation at 400 nm and emission at 457 nm. [substrate] = 5 μM. Slit widths were 3/3 nm. Decreases in the fluorescence intensity of 9-aminoacridine (5 μM) measured under identical conditions are compared (triangles).

Table 1. Fluorescence decay times of Cu-1 and Cu-2 complexes in the presence of varying concentration of DNA. Sample was excited by nano LED 404 and emission at 457 nm. Silt widths are 4 nm for both excitation and emission
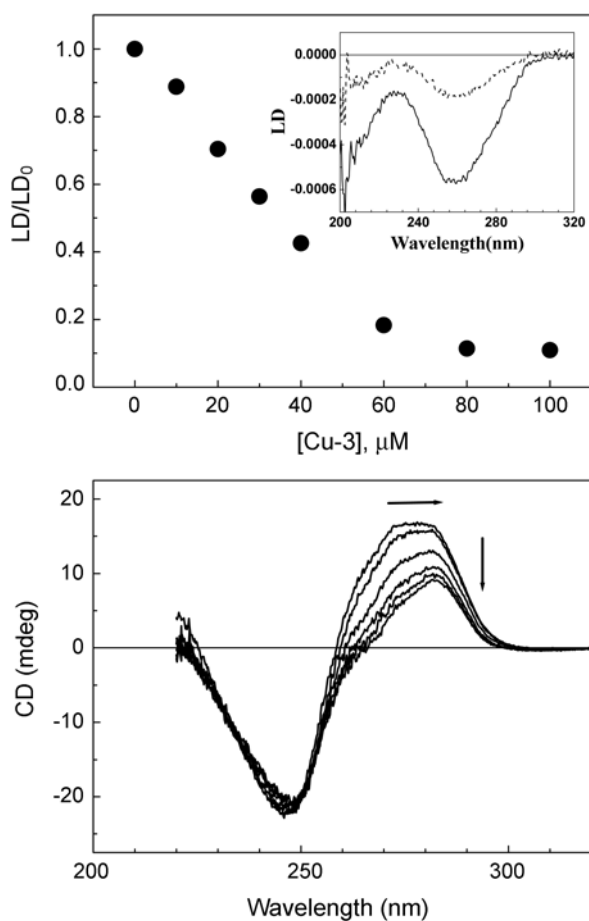
[DNA], μM	Cu-1 complex		Cu-2 complex	
	τ_1	a_1	τ_1	a_1
	τ_2	a_2	τ_2	a_2
0	0.11	56.20	0.10	36.58
	12.33	43.80	13.13	63.42
10	0.13	41.62	0.12	26.53
	12.60	58.38	13.36	73.47
20	0.27	25.88	0.16	16.02
	13.27	74.12	13.48	83.98
30	0.39	23.76	0.28	13.77
	13.34	76.24	13.62	86.23
40	0.49	26.45	0.37	16.83
	13.23	73.55	13.45	83.17
50	0.52	27.74	0.40	19.46
	13.10	72.26	13.48	80.54

Figure 4. LD^r spectrum of the 9-aminoacridine-DNA complex (dashed) in panel a, the Cu-1-DNA (dashed, curve a) and Cu-2-DNA (dotted, curve b) complex in panel b. That of the substrate-free DNA is shown as solid curves in panels a and b. [DNA] = 100 μM, [substrate] = 10 μM.

complexes are in the range of 3-5% that of 9-aminoacridine. A decrease in the fluorescence intensity of 9-aminoacridine upon binding to DNA has been well-documented.[21] The fluorescence intensities of both Cu-1 and Cu-2 complexes also decreased in the presence of DNA (Figure 3). However, in contrast with 9-aminoacridine, the fluorescence of Cu-1 and Cu-2 complexes do not completely disappear. Above the complex to DNA concentration ratio of 0.25, the decrease is almost proportional to the DNA concentration, while below the ratio of 0.25, the decrease stopped and the change reached a plateau, indicating that the substrate is saturated at the drug to DNA concentration ratio of 0.25. Fluorescence decay times of Cu-1 and Cu-2 complexes in the presence and absence of DNA are summarized in Table 1. The fluore-scence decay time of 9-aminoacridine was ~13.9 ns, while that of Cu-1 and Cu-2 complexes exhibits two decay compo-nents being ~0.10 ns and ~13.0 ns. The relative amplitudes of the short component are 56.2% and 36.6%, respectively, for Cu-1 and Cu-2 complexes, again indicating a strong interaction between the 9-aminoacridine and Cu(II)-tacn complex. As the DNA concentration increases thus, the drug to DNA concentration ratio decreases, the decay time of the short component showed a tendency to become longer while its amplitude decreased. Coincidently with the fluorescence intensity measurement, the decrease in the amplitude of the short decay time component reaches a plateau at the DNA concentration of 20 μM, corresponding to the substrate : DNA concentration ratio of 0.25. At a ratio below 0.25 (DNA concentration above 20 μM), the amplitudes of both Cu-1 and Cu-2 complexes of the long and short decay times do not change.

LD^r spectrum of the compound 1 and 2 complexed with DNA. The LD^r spectra of the substrate-free DNA and of the 9-aminoacridine-DNA complex are depicted in Figure 4, panel a. The LD^r spectrum of DNA is negative and the magnitude in the DNA absorption region is wavelength-

independent as it is expected from our set-up.[23] When 9-aminoacridine is complexed with DNA, a small increase in the LD^r magnitude in the DNA absorption region is observ-ed, which is typical for intercalation, indicating unwinding and stiffening of DNA upon the substrate intercalation.[24]

The magnitude of LD^r signals in the substrate absorption region is somewhat larger than that in the DNA absorption region, which is also typical for an intercalated substrate. Although the appearance of LD^r in the substrate absorption region is wavelength-dependent, suggesting that the vibronic transition may tilt from the plane of the DNA base pairs, the overall magnitude of LD^r in the electric transition region (370 nm-440 nm) can be considered as wavelength-independent. The overall shape of LD^r spectrum of Cu-1-DNA and Cu-2-DNA complexes appears to be similar to that of the 9-aminoacridine-DNA complex (Figure 4, panel b), suggesting that the angle of the acridine moiety with respect to the DNA helix axis is similar for all substrates examined in this work. However, there are several differences worth noting. The magnitudes of the LD^r spectrum in the DNA absorption region decrease upon binding of both Cu-1 and Cu-2 complexes. The decrease is more pronounced for Cu-2 complex. A decrease in LD^r magnitude of the DNA absorption region may reflect decrease in the orientability of DNA, which is one of the two factors determining the LD^r magnitude. The other factor, namely the optical factor, may be the same for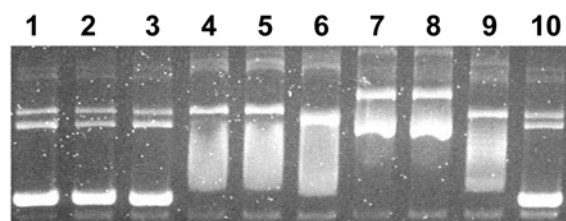 all three complexes: the chromophores in this absorption region namely, acridine and DNA bases, are in the similar condition.

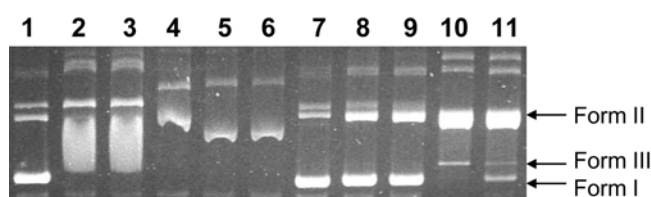**Changes in CD and LD in the presence of Cu-3 complex.** Cu-3 complex does not possess any aromatic moiety and, consequently, it is not active in the electric transition. Even when it forms a complex with Cu(II), neither metal to ligand charge transfer (MLCT) nor ligand-field transition band appear in the entire Uv/vis region, probably due to the low extinction coefficient. However, in the presence of Cu-3 complex, significant alternations in the CD and LD spectra of DNA itself are observed, indicating that this compound indeed associates with DNA (Figure 5). The intensity of LD at 260 nm decreases with an increasing concentration of Cu-3 complex (Figure 5, panel a). The decrease reaches a plateau when the drug-DNA concentration ratio reaches 0.25-0.3. However, the shapes of the LD signal and absorption spectrum do not change in the presence of Cu-3 complex (Figure 5, panel a, insertion) indicating that the presence of Cu-3 complex only affects the orientability of DNA, not the structure of nucleo-bases. The CD spectrum shows a decrease in CD intensity 260 nm-300 nm (Figure 5, panel b). At the highest Cu-3 complex concentration, although a significant alteration is observed, the characteristics of the B form CD spectrum is still conserved, suggesting that the arrangement of the DNA bases is somewhat altered.

Scissoring DNA by Cu(II)-tacn complexes. Figure 6 depicts the gel electrophoretic separations showing the binding of plasmid pCMV-Myc DNA induced by three ligands at different concentrations under identical conditions. From the top of lane 1-3, DNA in the presence of 9-aminoacridine shows the same band as the control (lane 10), corresponding to Form 1 (supercoiled DNA), suggesting that 9-aminoacridine does not cleave DNA. The migration speed of DNA in the absence and the presence of 9-aminoacridine are about the same. However, in the presence of ligands 1 (lanes 4-6) and 2 (lanes 7-9), the electrophoretic results in Figure 6 are very different from those mentioned above. A band broadening is apparent. Binding equilibrium occurs in less than an hour and the band intensities and patterns do not change within hours monitored (15 hr).

As shown in Figure 7, the gel electrophoretic separations with ligands 1 and 2 in the presence of Cu(II) ions, are almost the same as those in the absence of the Cu(II) ions. In

Figure 5. Decrease in LD intensity at 260 nm with increasing concentration of Cu-3 (panel a) and the CD spectrum in the presence of various concentrations of Cu-3 (panel b). LD intensity in the absence of Cu-3 is normalized to unity. LD spectrum in the absence (solid curve) and presence (dotted curve) of 30 μM Cu-3 are compared in the insertion. [DNA] = 100 μM.

Figure 6. Incubation (15 hr) of supercoiled DNA with ligands: Lane 1: DNA (114 mM) + Lanes 1-3: 50, 30, 10 mM of 9-aminoacridine, Lanes 4-6: 50, 30, 10 mM of **1**, Lanes 7-9: 50, 30, 10 mM compound **2**, Lane 10: DNA only: I = 10 mM NaNO$_3$, at pH 7.3 (10 mM HEPES) and 30 °C.

Figure 7. Incubation (15 hr) of supercoiled DNA with ligands + Cu(NO₃)₂: DNA (102 mM) + Lane 1: 20 mM of 9-aminoacridine + 40 mM Cu(NO₃)₂/Lanes 2-3: 20 mM of **1** + 20, 40 mM Cu(NO₃)₂/ Lanes 4-6: 20 mM of **2** + 10, 20, 40 mM Cu(NO₃)₂/Lane 7: DNA only/Lanes 8-11: 10 mM of **3** + 0, 10, 20, 40 mM of Cu(NO₃)₂: I = 10 mM NaNO₃, at pH 7.3 (10 mM HEPES) and 30 °C.

contrast, acridine-free ligand 3 shows clean three bands corresponding to Form I, III and Form II(from bottom to top in lane 11) in the presence of Cu(II) ions.

Discussion

Conformation of Cu-1, 2 and 3 complexes bound to DNA. In aqueous solution, the spectral properties, including absorption, fluorescence excitation and emission of both Cu-1 and Cu-2 complexes differ from those of 9-aminoacridine. This observation indicates that the environment of both the ground and excited states of the acridine chromophore are different. Since the structure of acridine moiety remains, the difference in spectral properties indicates a strong interaction between the acridine moiety and the Cu(II)-tacn complex. The coordination of the N atom in the acridine ring to the Cu^{2+} metal ion is one of the possibilities. However, the spectral properties of 9-aminoacridine, including Uv/vis spectrum, remains in the presence of Cu-3 complex (data not shown), indicating that the coordination requires the linker. Upon binding to DNA, there occurred a strong red-shift and hypochromicity in the absorption band of the acridine chromophore. These spectral changes indicate that the acridine moiety of all three compounds intercalates. A large red-shift observed for the groove binder usually correlates with a substrate conformation change on binding or substrate-substrate interaction can be expected because the acridine moiety is rigid and the substrate to DNA concentration is low. The stoichiometry observed from fluorescence titration - that saturation occurred at a substrate to DNA concentration ratio of 0.25-0.3 for Cu-1 and Cu-2 complexes, supports the nearest neighbor exclusion model of intercalation.

The LD^r with its magnitude in the substrate absorption region larger than that in the DNA absorption region also indicates the intercalation of the acridine moiety.[22-24] The decrease in LD^r magnitude in the DNA absorption region that is observed for the Cu-1-DNA and Cu-2-DNA complexes indicates that the DNA stem is bent. Another possibility that partial dissociation of the double-stranded DNA that also results in increasing the flexibility of DNA is not likely, because the binding of 9-aminoacridine increases the melting temperature of double-stranded DNA.[25] Assuming that the acridine transition moments are perpendicular to the flow direction, the tilt angle of the DNA base near the binding site

relative to the acridine molecular plane can be calculated.[24] These angles were calculated as 76°, 72° and 60° for the 9-aminoacridine-DNA, Cu-1-DNA and Cu-2-DNA complex, respectively. The largest tilt angle observed for the Cu-2-DNA complex is not surprising because the steric perturbation due to the binuclear Cu(II)-tacn complex, which prefers to interact with the phosphate group of DNA, would be largest for Cu-2 complex.

Binding of Cu-3 complex resulted in the decrease of the LD and LD^r magnitude hence, enhancement of DNA flexibility. This observation may rule out the possibility of the Cu-3 complex intercalation. When intercalation of any substrate occurs, elongation and increase in the stiffness of DNA is expected which will result in increased LD and LD^r magnitude. The repulsion between phosphate groups may decrease upon binding of Cu(II)-tacn complex which is positively charged, thereby increasing the flexibility of DNA, which results a decreased LD magnitude.

DNA cleavage. Spectroscopic studies suggest that the 9-aminoacridine moiety is intercalated into DNA bases. On the agarose gel picture, DNA with 9-aminoacridine seems to migrate as almost the same speed as DNA control (lanes 1-3 and 10, in Fig. 6). DNA incubated with ligands 1 and 2 migrates very slowly with a distinct binding pattern.

In the presence of Cu(II) ion, ligand 3, which does not have 9-aminoacridine moiety, shows DNA cleavage, producing form II, and form III (lanes 8-11 in Fig. 7). As binding study suggested, the Cu-3 complex directly interacts with phosphates and cleaved DNA stepwise. It has been reported that the Cu-3 complex mediated hydrolysis of DNA was 30 times faster than the corresponding mononuclear Cu-tacn complex. The cooperative role of two Cu(II) ions in the Cu-3 complex was suggested to play a key role in cleaving DNA.[16]

In the presence of Cu(II) ion, the binding pattern of 9-aminoacridine, 1, and 2 do not change as in the absence of Cu(II) ion (Fig. 7). It is not clear whether the broad bands in lanes 2-6 in Figure 7, correspond to nicked DNA (Form II) or due to slow migration upon nonspecific binding. It is not likely due to the binding with the cleavage product, linearized DNA (Form III). In separate experiments performed with the linearized DNA (data not shown), the gel mobility shift pattern is different from the above. There is no indication of cleavage of Form III DNA by any of four Cu complexes since absorbance intensities of the DNA/Cu-complex adducts in the gel remain the same under the conditions used. A few acridine conjugated mononuclear Cu(II) complexes have been reported to produce rather distinct bands in the gel, showing some DNA cleavage to form nicked DNA,[18] unlike the Cu-1 and Cu-2 complexes.

Cu-1 and Cu-2 complexes seem tightly bind to DNA through acridine moiety according to binding studies. Binding patterns with DNA in the gel could be attributed from charge difference between mononuclear vs binuclear Cu(II) center. In terms of nuclease reactivity, Cu centers in both Cu-1 and Cu-2 complexes might not be in right juxtaposition for cleaving DNA phosphate backbone.

We expected that attaching intercalator to binuclear ligand

3 would enhance the catalytic efficiency in cleaving DNA. However, the results suggest that introduction of intercalator likely limits the orientation of the Cu center, slowing down the catalytic process. Linkers between the metal complex and acridine moiety may play important role in DNA cleavage reaction.

References

1. *Metal Ions in Biological System*; Sigel, A.; Sigel, H., Eds.; Macel Dekker; New York, 1996.
2. Pratvicl, G.; Bernadou, J.; Mcunicr, B. *Adv. Inorg. Chem.* **1998**, *45*, 251.
3. Ji, L.-N.; Zou, X.-H.; Liu, J.-G. *Coord. Chem. Rev.* **2001**, *216-217*, 143.
4. Cowan, J. A. *Curr. Opin. Chem. Biol.* **2001**, *5*, 634.
5. Sigman, D. S.; Graham, D. R.; Aurora, V. D.; Stern, A. M. *J. Biol. Chem.* **1979**, *254*, 12269.
6. Detmer III, C. A.; Pamatong, F. V.; Bocarsly, J. R. *Inorg. Chem.* **1997**, *36*, 3676.
7. Ahsan, H.; Hadi, S. M. *Cancer Lett.* **1998**, *124*, 23.
8. Liu, J.; Zhang, T.; Lu, T.; Qu, L.; Zhou, H.; Zhang, Q.; Ji, L. *J. Inorg. Biochem.* **2002**, *91*, 269.
9. Vaidyanathen, V. G.; Nair, B. U. *J. Inorg. Biochem.* **2003**, *93*, 271.
10. Benites, P. J.; Holmberg, R. C.; Rawat, D. S.; Kraft, B. J.; Klein, L. J.; Peters, D. G.; Thorp, H. H.; Zaleski, J. M. *J. Am. Chem. Soc.* **2003**, *125*, 6434.
11. González-Álvarez, M.; Alzuet, G.; Borrás, J.; Pitié, M.; Meunier, B. *J. Biol. Inorg. Chem.* **2003**, *8*, 644.
12. Wang, X.-L.; Chao, H.; Li, H.; Hong, X.-L.; Ji, L.-N.; Li, X.-Y. *J. Inorg. Biochem.* **2004**, *98*, 423.
13. Thomas, A. M.; Nethaji, M.; Chakravarty, A. R. *J. Inorg. Biochem.* **2004**, *98*, 1087.
14. Reddy, P. R.; Rao, K. S.; Satyanarayana, B. *Tetrahedron Lett.* **2006**, *47*, 7311.
15. Hegg, E. L.; Burstyn, J. N. *Inorg. Chem.* **1996**, *35*, 7474.
16. Kim, J. H.; Kim, S. H. *Chem. Lett.* **2003**, *32*, 490.
17. Kim, J. H. *Bull. Korean. Chem. Soc.* **2004**, *25*, 410.
18. Hirohama, T.; Arii, H.; Chikira, M. *J. Inorg. Biochem.* **2004**, *98*, 1778.
19. Hansen, J. B.; Koch, T.; Buchardt, O.; Nielsen, P. E.; Wirth, M.; Nordén, B. *Biochemistry* **1983**, *22*, 4878.
20. Kim, H.-K.; Kim, J.-M.; Kim, S. K.; Rodger, A.; Nordén, B. *Biochemistry* **1996**, *35*, 1187.
21. Kim, H.-K.; Cho, T.-S.; Kim, S. K. *Bull. Korean. Chem. Soc.* **1996**, *17*, 358.
22. Benesi, H. A.; Hildebrand, J. H. *J. Am. Chem. Soc.* **1949**, *71*, 2703.
23. Nordén, B.; Rodger, A. *Circular Dichroism and Linear Dichroism*; Oxford University Press: London, UK, 1997.
24. Eimer, T.; Nordén, B. *Bioorg. Med. Chem.* **1995**, *3*, 701.
25. Hyun, H.-M.; Lee, G.-J.; Cho, T.-S.; Kim, S. K.; Yi, S. Y. *Bull. Korean Chem. Soc.* **1997**, *18*, 528.